Supporting Information for

Tris(dimethylamino)silylium ion: structure and reactivity of a dimeric silaguanidinium

Nina Kramer, Hubert Wadepohl, Lutz Greb*

Department of Inorganic Chemistry, Ruprecht-Karls-University, Heidelberg, Germany.

1. Experimental Details

1.1. Materials and General Methods

Unless otherwise stated, all manipulations were carried out under a dry argon atmosphere by using standard Schlenk techniques to prevent hydrolysis of the sensitive compounds. All solvents were rigorously dried by applying standard procedures, freshly degassed and stored over molecular sieve (3 Å resp. 4 Å) prior to use. All glassware, syringes, magnetic stirring bars and needles were thoroughly dried. The commercially available chemicals $(Me_2N)_3SiH$, $OPEt_3$, 1-methylindole, ferrocene, *N,N*-dimethylaniline and $[Ph_3C][BArF_{20}]$ (= $[Ph_3C][B(C_6F_5)_4]$) were used as received. All compounds were stored in a glove box (MBraun LABmaster dp, MB-20-G) under N_2 atmosphere. Purity and identity of the compounds were confirmed by high resolution multinuclear NMR-spectroscopy, mass spectrometry and if possible, X-ray diffraction analysis. Elementary analysis was performed on vario EL and vario MICRO cube from Elementar Analysensysteme GmbH. ^{1}H-, ^{13}C- and ^{29}Si-NMR spectra were collected with a Bruker Advance II 400 or Bruker Advance III 600 NMR spectrometer and referenced to tetramethylsilane. Chemical shifts are reported as dimensionless δ values, coupling constants J are given in hertz (Hz). Electrospray ionization mass spectra were obtained with a Bruker ApexQe FT-ICR instrument, LIFDI spectra were recorded with JEOL JMS-700 magnetic sector.

2. Syntheses

2.1. $[(NMe_2)_3Si]_2$ $[(B(C_6F_5)_4)_2]$ / [1] $[(B(C_6F_5)_4]_2$

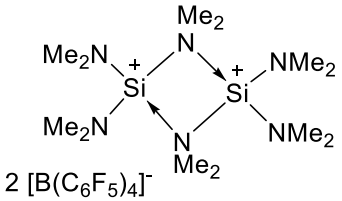

2.13 g (2.31 mmol, 1.00 eq.) $[Ph_3C][B(C_6F_5)_4]$ were dissolved in 10.0 mL *o*-dichlorobenzene. To the bright yellow solution, 0.37 g (2.30 mmol, 1.00 eq.) $(NMe_2)_3SiH$ were slowly added at room temperature. The solution was stored over night at room temperature. The color of the solution faded to yellowish and colorless crystals precipitated. The crude product was washed with small amounts of *n*-pentane. After drying, the pure product was obtained as colorless powder, yielding 1.23 g (1.47 mmol, 64%).

^{1}H-NMR (400 MHz, *o*-difluorobenzene) δ 3.67 (s, 6H, bridged N(C*H*$_3$)$_2$, *H*$_2$), 3.20 (s, 12H, terminal N(C*H*$_3$)$_2$, *H*$_1$).

^{13}C{^{1}H}-NMR (150 MHz, *o*-difluorobenzene) δ 44.1 (bridged N(*C*H$_3$)$_2$), 37.4 (terminal N(*C*H$_3$)$_2$).

^{1}H/^{29}Si-HMBC (79 MHz, *o*-difluorobenzene) δ -30.6.

^{15}N-HMBC (600 MHz, *o*-difluorobenzene) δ 49.1 (terminal *N*(CH$_3$)$_2$, bridged *N*(CH$_3$)$_2$ not visible.

^{11}B-NMR (129 MHz, *o*-difluorobenzene) δ -16.2.

^{19}F-NMR (376 MHz, *o*-difluorobenzene) δ-132.5 (d, $^{3}J_{FF}$ = 11.3 Hz, 2F, F$_{ortho}$), -163.7 (t, $^{3}J_{FF}$ = 21.7 Hz, 1F, F$_{para}$), -167.6 (t, $^{3}J_{FF}$ = 21.7 Hz, 2F, F$_{meta}$).

^{1}H-NMR (400 MHz, dichloromethane-*d*$_2$) δ 3.22 (s, 6H, bridged N(C*H*$_3$)$_2$, *H*$_2$), 2.58 (s, 12H, terminal N(C*H*$_3$)$_2$), *H*$_1$).

^{1}H/^{29}Si-HMBC (79 MHz, dichloromethane-d$_2$) δ -31.3.

^{11}B-NMR (129 MHz, dichloromethane-d$_2$) δ -16.7.

^{19}F-NMR (376 MHz, dichloromethane-d$_2$) δ -133.1 (d, $^{3}J_{FF}$ = 11.3 Hz, 2F, F$_{ortho}$), -166.4 (t, $^{3}J_{FF}$ = 21.7 Hz, 1F, F$_{para}$), -167.1 (t, $^{3}J_{FF}$ = 21.7 Hz, 2F, F$_{meta}$).

MS (ESI+) $\frac{m}{z}$ calculated for $C_6H_{18}N_3Si^+$ = 160.13; found 160.13.

Elemental analysis calculated C 43.93, H 2.16, N 5.01; found C 43.36, H 2.54, N 4.92.

Crystals suitable for X-Ray diffraction analysis were obtained by performing the reaction in toluene-*d*$_8$ and dissolving the resulting oil in dichloromethane-*d*$_2$ or directly from the *o*-dichlorobenzene solution.

To verify its stability, [1][(B(C$_6$F$_5$)$_4$]$_2$ was dissolved in mixtures of *o*-difluorobenzene (to ensure full solubility) with benzene, toluene, fluorobenzene or dichloromethane. No decomposition at room temperature was observed.

The ^{1}H chemical shift of the dimer depends on the additional solvent (Fig. SI 17, table 1).

Table SI1: Chemical shifts of [1][(B(C$_6$F$_5$)$_4$]$_2$ in different solvents.

	o-difluorobenzene	*o*-difluorobenzene + benzene	*o*-difluorobenzene + toluene	*o*-difluorobenzene + fluorobenzene	*o*-difluorobenzene + dichloromethane
^{1}H-NMR	3.67, 3.20	3.11, 2.79	3.21, 2.85	3.44, 2.98	3.45, 2.98
^{29}Si/^{1}H-HMBC-NMR	-30.6	-32.15	-31.3	-31.8	-31.4

2.2. $[(NMe_2)_3Si(OPEt_3)][B(C_6F_5)_4]$

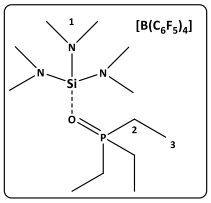

30.0 mg ($1.79 \cdot 10^{-5}$ mmol, 1.00 eq.) of [1][$(B(C_6F_5)_4]_2$ were suspended in 0.50 mL dichloromethane-d_2. 4.80 mg ($3.58 \cdot 10^{-5}$ mmol, 2.00 eq) $OPEt_3$ were added to the colorless solution. The reaction was stored for 5 min.

^{1}H-NMR (400 MHz, dichloromethane-d_2) δ 2.49 (s, 18 H, H_1), 2.13 (dq, $^2J_{PH}$ = 11.5 Hz, 6H, H_2), 1.29 (dt, $^3J_{PH}$ = 19.5 Hz, 9H, H_3).

^{13}C{^{1}H}-NMR (150 MHz, dichloromethane-d_2) δ 37.3 (C_1), 17.9 (d, $^1J_{P-C}$ = 65.8 Hz, C_2), 5.1 (d, $^2J_{PC}$ = 5.6 Hz, C_3).

^{1}H/^{29}Si-HMBC (79 MHz, dichloromethane-d_2) δ -44.8.

^{11}B-NMR (129 MHz, dichloromethane-d_2) δ -16.7.

^{19}F-NMR (376 MHz, dichloromethane-d_2) δ -133.1 (d, 2F, $^3J_{FF}$ = 11.3 Hz, F_{ortho}), -163.7 (t, 1F, $^3J_{FF}$ = 21.7 Hz, F_{para}), -167.5 (t, 2F, $^3J_{FF}$ = 21.7 Hz, F_{meta}).

^{31}P-NMR (162 MHz, dichloromethane-d_2) δ 85.2.

MS (ESI+) $\frac{m}{z}$ calculated for $C_{12}H_{33}N_3SiOP^+$ = 294.21; obtained 294.21.

In an independent experiment, the cation of [2], $[(NMe_2)_3Si(OPEt_3)]^+$, was synthesized by reacting 34.1 mg ($1.10 \cdot 10^{-4}$ mmol, 1.00 eq.) $[(NMe_2)_3Si][OTf]$ with 14.8 mg ($1.10 \cdot 10^{-4}$ mmol, 1.00 eq) $OPEt_3$ in toluene-d_8 for 5 min. The compound directly crystallized from solution and the connectivity could be confirmed by Xray diffraction.

^{1}H-NMR (400 MHz, toluene-d_8) δ 2.26 (s, 18 H, H_1), 1.18 (dq, $^2J_{PH}$ = 11.5 Hz, 6H, H_2), 0.88 (dt, $^3J_{PH}$ = 19.5 Hz, 9H, H_3).

^{13}C{^{1}H}-NMR (150 MHz, toluene-d_8) δ 36.9 (C_1), 17.6 ($^1J_{P-C}$ = 65.8 Hz, C_2), 4.8 (d, $^2J_{P-C}$ = 5.6 Hz, C_3).

^{1}H/^{29}Si-HMBC (79 MHz, toluene-d_8) δ -46.7.

^{19}F-NMR (376 MHz, toluene-d_8) δ -77.9 (s, F_{OTf}).

^{31}P-NMR (162 MHz, toluene-d_8) δ 89.9.

^{1}H-NMR (400 MHz, dichloromethane-d_2) δ 2.48 (s, 18 H, H_1), 2.29 (dq, $^2J_{PH}$ = 11.5 Hz, 6H, H_2), 1.28 (dt, $^3J_{PH}$ = 19.5 Hz, 9H, H_3).

^{1}H/^{29}Si-HMBC (79 MHz, dichloromethane-d_2) δ -46.1.

^{19}F-NMR (376 MHz, dichloromethane-d_2) δ -79.0 (s, F_{OTf}).

^{31}P-NMR (162 MHz, dichloromethane-d_2) δ 87.5.

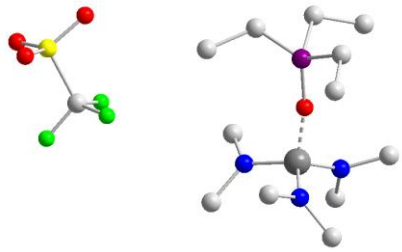

Molecular structure of $[(NMe_2)_3Si(OPEt_3)][OTf]$ (only connectivity was established)

2.3. Ferrocenyl-(bis-dimethylamino)(dimethylammonium)silyl $[(B(C_6F_5)_4]$ / [2a]$[(B(C_6F_5)_4]$

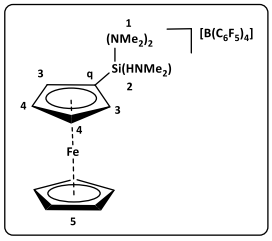

24.7 mg ($1.47 \cdot 10^{-5}$ mmol, 1.00 eq.) of $[1][(B(C_6F_5)_4]_2$ were suspended in 0.50 mL dichloromethane-d_2. 5.45 mg ($2.94 \cdot 10^{-5}$ mmol, 2.00 eq.) ferrocene were added to the reaction mixture. An orange solution formed, of which ^{1}H-NMR spectroscopy indicated full conversion to one product. Layering of the solution with *n*-pentane yielded yellow crystals overnight.

^{1}H-NMR (400 MHz, dichloromethane-d_2) δ 4.66 (t, 2H, H_3), 4.45 (s, 1H, H_2), 4.27 (s, 5H, H_5), 4.22 (t, 2H, H_4) 2.77 (s, 18H, $H_{1,2}$).

^{13}C{^{1}H}-NMR (150 MHz, dichloromethane-d_2) δ 75.1 (C_3), 74.5 (C_4), 69.9 (C_5), 55.6 (C_q), 38.6 ($C_{1,2}$).

^{1}H/^{29}Si-HMBC (79 MHz, dichloromethane-d_2) δ -11.7.

^{11}B-NMR (129 MHz, dichloromethane-d_2) δ -16.7 (s).

^{19}F-NMR (376 MHz, dichloromethane-d_2) δ -133.1 (d, $^3J_{FF}$ = 11.3 Hz, F_{ortho}), -163.7 (t, $^3J_{FF}$ = 21.7 Hz, F_{para}), -167.5 (t, $^3J_{FF}$ = 21.7 Hz, F_{meta}).

MS (LIFDI+) $\frac{m}{z}$ calculated for $C_{16}H_{28}FeN_3Si^+$ = 346.14; obtained 346.12.

2.4. 1-Methyl-3-(bis-dimethylamino)(dimethylammonium)silylindole $[(B(C_6F_5)_4]$ / [2b] $[(B(C_6F_5)_4]$

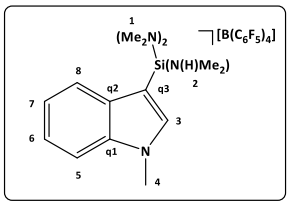

20.0 mg ($1.19 \cdot 10^{-5}$ mmol, 1.00 eq.) of $[1][(B(C_6F_5)_4]_2$ were suspended in 0.50 mL dichloromethane-d_2. 3.20 mg ($2.38 \cdot 10^{-5}$ mmol, 2.00 eq.) 1-methylindole were added to the reaction mixture. ^{1}H-NMR spectroscopy indicated full conversion to one product. To remove solvent impurities, the product was washed with *n*-pentane and toluene.

^{1}H-NMR (400 MHz, dichloromethane-d_2) δ 7.49 (dt, $^{3}J_{HH}$ = 7.7 Hz, 2H, $H_{8,5}$), 7.39 (s, 1H, H_3), 7.38 (dt, $^{3}J_{HH}$ = 7.7 Hz, 1H, H_7), 7.28 (dt, $^{3}J_{HH}$ = 7.7 Hz, 1H, H_6), 4.45 (bs, 1H, N*H*), 3.88 (s, 3H, H_4), 2.78 (d, $^{4}J_{HH}$ = 5.3 Hz, 6H, H_2), 2.75 (s, 12H, H_1).

^{13}C{^{1}H}-NMR (150 MHz, dichloromethane-d_2) δ 140.6 (C_3), 139.3 (C_{q1}), 131.5 (C_{q2}), 123.9 (C_7), 122.5 (C_6), 121.7 (C_8), 111.4 (C_5), 93.6 (C_{q3}), 38.6 (C_2), 36.8 (C_1), 33.9 (C_4).

^{1}H/^{29}Si-HMBC (79 MHz, dichloromethane-d_2) δ -16.9.

^{11}B-NMR (129 MHz, dichloromethane-d_2) δ -16.7.

^{19}F-NMR (376 MHz, dichloromethane-d_2) δ -133.1 (d, $^{3}J_{FF}$ = 11.3 Hz, F_{ortho}), -163.5 (t, $^{3}J_{FF}$ = 21.7 Hz, F_{para}), -167.5 (t, $^{3}J_{FF}$ = 21.7 Hz, F_{meta}).

MS (LIFDI+) $\frac{m}{z}$ calculated for $C_{15}H_{27}N_4Si^+$ = 291.20; obtained 291.19.

2.5. *N,N*-dimethyl-4-(bis-dimethylamino)(dimethylammonium)silylbenzamine [(B(C$_6$F$_5$)$_4$)] / [2c] [(B(C$_6$F$_5$)$_4$)]

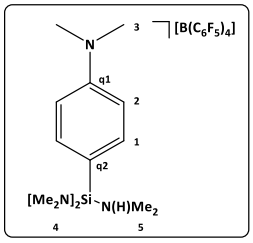

29.2 mg (1.73·10^{-5} mmol, 1.00 eq.) of [1][(B(C$_6$F$_5$)$_4$]$_2$ were suspended in 0.50 mL dichloromethane-d_2. 4.2 mg (3.49·10^{-5} mmol, 2.00 eq.) *N,N*-dimethylaniline were added to the reaction mixture. A colorless solid precipitated, but slowly dissolved overnight. ^{1}H-NMR spectroscopy indicated full conversion to one product. To remove solvent impurities, the product was washed with *n*-pentane and toluene.

^{1}H-NMR (400 MHz, dichloromethane-d_2) δ 7.35 (d, $^{3}J_{HH}$ = 9.18 Hz, 2H, H_1), 6.77 (d, $^{3}J_{HH}$ = 9.18 Hz, 2H, H_2), 3.02 (s, 6H, H_3), 2.83 (bs, 6H, H_5), 2.71 (s, 12H, H_4).

^{13}C{^{1}H}-NMR (150 MHz, dichloromethane-d_2) δ 153.7 (C_{q1}), 137.0 (C_1), 112.6 (C_2), 106.1 (C_{q2}), 40.0 (C_2), 38.7 (C_4), 38.2 (C_5).

^{1}H/^{29}Si-HMBC (79 MHz, dichloromethane-d_2) δ -15.5.

^{11}B-NMR (129 MHz, dichloromethane-d_2) δ -16.7.

^{19}F-NMR (376 MHz, dichloromethane-d_2) δ -133.1 (d, $^{3}J_{FF}$ = 11.3 Hz, F_{ortho}), -163.5 (t, $^{3}J_{FF}$ = 21.7 Hz, F_{para}), -167.5 (t, $^{3}J_{FF}$ = 21.7 Hz, F_{meta}).

MS (LIFDI+) $\frac{m}{z}$ calculated for $C_{14}H_{29}N_4Si^+$ = 281.22; obtained 281.20.

3. Catalysis section

3.1. 1-Fluoroadamantane

8.5 mg ($5.51 \cdot 10^{-5}$ mmol, 1.00 eq.) of 1-fluoroadamantane and 9.5 mg ($8.17 \cdot 10^{-5}$ mmol, 1.40 eq.) of Et_3SiH were dissolved in 0.50 mL *o*-diflurorbenzene. 5.6 mg ($3.33 \cdot 10^{-6}$ mmol, 6 mol%) of $[1][(B(C_6F_5)_4]_2$ were added to the reaction mixture. 50% conversion was observed after 30 min by ^{19}F-NMR peak integration of 1-fluoroadamantane vs. Et_3SiF (solvent signal as internal standard), and >95% conversion to adamantane in <12 h.

^{1}H-NMR (400 MHz, *o*-diflurorbenzene) δ 3.79 (s, 1H, $Et_3Si\mathit{H}$), 2.71 (s, $N\mathit{Me}_2$), 1.88 (bs, 4H, Ad), 1.81 (bs, 12H, Ad), 1.04 (m, 28H, Et_3SiH and Et_3SiF), 0.68 (m, 19H, Et_3SiH and Et_3SiF).
^{1}H/^{29}Si-HMBC (79 MHz, *o*-diflurorbenzene) δ 32.7 (Et_3SiF), 0.0 ($Et_3\mathit{Si}H$).
^{19}F-NMR (376 MHz, *o*-diflurorbenzene) δ -132.4 (d, $^3J_{FF}$ = 11.3 Hz, F_{ortho}), -163.8 (t, $^3J_{FF}$ = 21.7 Hz, F_{para}), -167.6 (t, $^3J_{FF}$ = 21.7 Hz, F_{meta}), 175.7 ($Et_3Si\mathit{F}$).

4. Computational section

Geometry and energies → DLPNO-CCSD(T)/cc-pVQZ//PW6B95-D3(BJ)/def2-TZVPP

Geometry optimizations and single point energy calculations have been performed with ORCA 4.1.[1] The RI approximation[2] for the Coulomb integrals was used in all cases (RIJCOSX), with application of corresponding auxiliary basis sets.[3] PW6B95[4] including Grimme's semi-empirical dispersion correction[5] with Becke-Johnson damping function[6] (D3(BJ) and the def2-TZVPP[7] basis set revealed best to reproduce the experimentally determined bond lengths. All calculated geometries have been confirmed as energetic minima on the potential energy surface by analytical calculation of harmonic frequencies at the BP86-D3(BJ)/def2-SVP level, revealing only positive values. Enthalpy and entropy corrections at 298 K have been calculated with the same level of theory by using the rigid-rotor harmonic oscillator (RRHO) approximation,[8] as implemented in ORCA. The final single point electronic energies were calculated with the highly accurate and linear scaling version of domain based localized pair natural orbitals based coupled cluster theory (DLPNO-CCSD(T)), as implemented in ORCA 4.1.[9] It has been shown that the DLPNO-CCSD(T) method reproduces experimentally obtained bond energies within an accuracy of around 3 kJ mol^{-1}.[10] NormalPNO and the default threshold settings were used. Dunning's augmented correlation consistent cc-pVQZ basis set and matching auxiliary basis sets were used.[11] As it can be expected with this basis set size, no extrapolation techniques or BSSE corrections are required for an accurate description.[12]

Solvent correction $\Delta G_{solv(COSMO\text{-}RS)}$: the corresponding free solvation enthalpy obtained from COSMO-RS[13] calculations as implemented in the ADF program package,[14] based on BP86-D3/TZ2P[15] single point energy calculations for the electrostatic solute-solvent interaction. With the COSMO-RS model accurate, δG_{solv} values with an error of about 1 kcal mol^{-1} for neutral molecules are usually obtained, but the estimated errors for charged species should be larger.[13c, 16] The dependency of the outcome of COSMO-RS on the DFT method has found to be very weak.[17]

Compound	E [H] BP86-D3/SVP D3 ORCA	AO?	in kJ	ther. corr [kcal]	Enthalpy [kJ]	enthalp< [kJ]	Gibbs correction	Gibbs in kJ	free energy [kJ]
Si(NMe2)3_kat	-692.7149	ok	-1818722.9	162.2	680.25	-1818042.6	128.5	537.1	-1818185.8
Si(NMe2)3_dikat	-1385.3983	ok	-3637363.3	326.8	1368.53	-3635994.7	275.5	1151.5	-3636211.8
2 x DMASi_kat						-3636085.288			-3636371.618
Dimerization						90.6			159.8
	E [H] PW6B95/TZVPP D3 ORCA		in KJ			summed H			summed G
	-693.9867		-1822062.1			-1821381.8			-1821525.0
	-1387.9297		-3644009.4			-3642640.9			-3642858.0
2 x DMASi_kat						-3642763.678			-3643050.008
Dimerization						122.8			192.1
	E [H] DLPNO-ccpVQZ		in KJ			summed H			summed G
	-692.0465		-1816968.0			-1816287.7			-1816430.9
	-1384.0535		-3633832.5			-3632464.0			-3632681.0
2 x DMASi_kat						-3632575.418			-3632861.748
Dimerization						111.4			180.7
			COSMO-RS [kcal]	COSMO-RS [kJ]					
deltaG_solv	Si(NMe2)3_kat		-45.03	-188.4					
	[Si(NMe2)3]_2_dikat		-141.5	-592.0					
				-215.2	final energy incl				
				in ODCB	solv. Correct	-103.8			-34.5

EDA → BP86-D3/TZ2P//PW6B95/def2-TZVPP

The EDA scheme arbitrarily decomposes the interaction energies (ΔE_{int}) between the *prepared* monomers into contributions of Pauli repulsion (ΔE_{Pauli}), electrostatic interaction (ΔE_{elstat}), orbital interaction (ΔE_{orb}) and dispersion (ΔE_{disp}). To obtain the final association energies (D_e) between the *relaxed* fragments, the preparation energies (ΔE_{prep}) have to be added to the interaction energies. The ΔE_{prep} include the energy necessary to prepare both fragments from their relaxed geometry to the geometry in the dimer. The intuitive fragmentation into two closed shell monomeric, cationic species was chosen, and the corresponding EDA values (based on BP86-D3/TZ2P) are given in table SI2.

Table SI 2: *Energies (kJ mol^{-1}) obtained by EDA (BP86-D3/TZ2P), percentages in parentheses give the contribution to the total interaction energy.*

ΔE_{int}	-257.57
ΔE_{Pauli}	1707.51
ΔE_{elstat}	-793 (40.4%)
ΔE_{orb}	-1065.01 (54.2%)
ΔE_{disp}	-107.07 (5.5%)
ΔE_{prep}	163.05
D_e	68.53

ETS-NOCV → BP86-D3/TZ2P// PW6B95/def2-TZVPP

The qualitative evaluation of the charge density deformation (NOCV)[19] as well as the quantitative description (ETS)[20] was performed as implemented in the ADF program package, choosing closed-shell fragments, employing the BP86-D3/TZ2P// PW6B95/def2-TZVPP level of theory. The dimers were fragmented into the closed shell species similar to the EDA, yielding NOCV deformation densities, which qualify and quantify the types of the orbital interactions for the dimerization process. A general description of the ETS-NOCV[21] can be found in the original literature. The orbital interaction term, ΔE_{Orb} is decomposed in different pairs of eigenvectors of the valence operator, and the particular types of bonds assigned by visual inspection of the shape of the deformation density, as well as by inspection of the corresponding contributing fragment donor and acceptor orbitals.

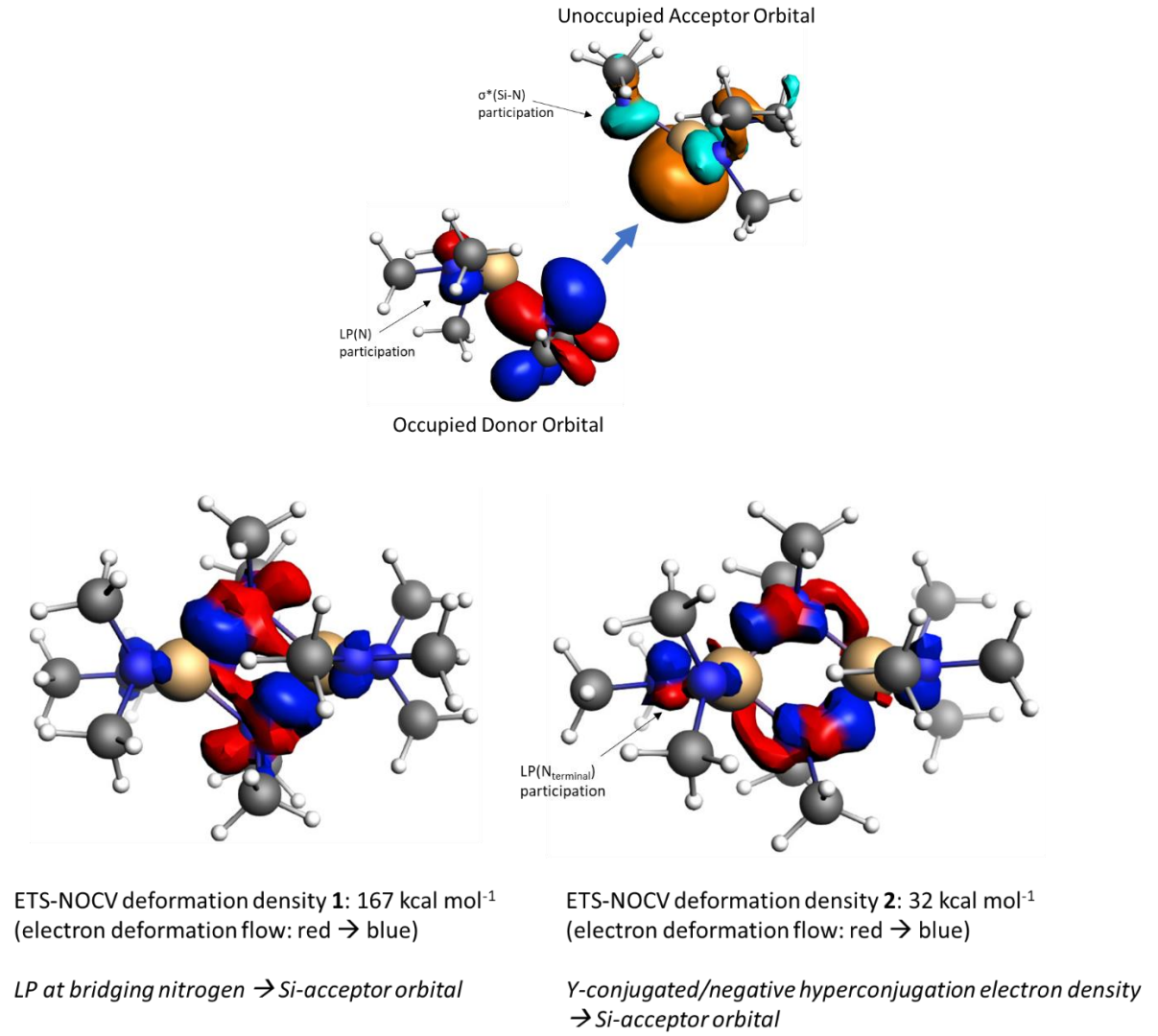

Figure SI1: ETS-NOCV derived deformation channels (bottom, red = charge depletion, blue = charge accumulation), together with the responsible occupied (oFMO) and unoccupied (uFMO) fragment molecular orbitals (top). Isosurface value for FMOs: 0.05; for NOCVs: 0.003 au.

5. X-Ray diffraction

General

Crystal data and details of the structure determinations are compiled in Table 2. Intensity data were collected at low temperature with an Enraf-Nonius Kappa CCD diffractometer (Mo-K_α radiation, sealed X-ray tube, graphite monochromator) or an Agilent Technologies Supernova-E CCD diffractometer (Cu-K_α radiation, microfocus X-ray tube, multilayer mirror optics). Detector frames from ω- and φ-scans were integrated by profile fitting.[25,26,27] Data were corrected for air and detector absorption, Lorentz and polarization effects[26,27] and scaled essentially by application of appropriate spherical harmonic functions.[28,29,30] Absorption by the crystal was treated with a semiempirical multiscan method and augmented by a spherical correction,[31] or numerically (Gaussian grid).[27,30,32] The structures were solved by intrinsic phasing[33] or by ab initio dual space methods involving difference Fourier syntheses (VLD procedure)[34] and refined by full-matrix least squares methods based on F^2 against all unique reflections.[35] All non-hydrogen atoms were given anisotropic displacement parameters. Hydrogen atoms were generally input at calculated positions and refined with a riding model.[36] When justified by the quality of the data the positions of some hydrogen atoms (those on the substituted cyclopentadiene ring) were refined. A split atom model was used to refine disordered solvent molecules. When found necessary, suitable geometry and adp restraints or constraints were applied.[36] CCDC 1915081 - 1915082 contains the supplementary crystallographic data for this paper. These data can be obtained free of charge from the Cambridge Crystallograhic Data Centre's and FIZ Karlsruhe's joint Access Service via https://www.ccdc.cam.ac.uk/structures/?.

Table SI 3: Details of the crystal structure determinations of [**1**][B(C_6F_5)$_4$)]$_2$·2CH_2Cl_2 and [2a][B(C_6F_5)$_4$)].

	[**1**][B(C_6F_5)$_4$)]$_2$·2CH_2Cl_2	**[2a]**[B(C_6F_5)$_4$)]
formula	$C_{62}H_{40}B_2Cl_4F_{40}N_6Si_2$	$C_{40}H_{28}BF_{20}FeN_3Si$
crystal system	monoclinic	monoclinic
space group	$P\ 2_1/c$	$P\ 2_1/n$
a /Å	17.9010(2)	9.990(2)
b /Å	22.8764(3)	18.213(4)
c /Å	17.21509(19)	22.061(4)
b /°	98.6215(11)	92.18(3)

	[**1**][B(C_6F_5)$_4$)]$_2$·2CH_2Cl_2	**[2a]**[B(C_6F_5)$_4$)]
V /Å^3	6970.08(14)	4011.0(14)
Z	4	4
M_r	1848.60	1025.40
F_{000}	3680	69147
d_c /Mg⋅m^{-3}	1.762	1.698
m /mm^{-1}	3.302	0.536
max., min. transmission factors	1.000, 0.590 [a]	0.7460, 0.6357 [b]
X-radiation, *l* /Å	Cu-*K*a, 1.54184	Mo-*K*a, 0.71073
data collect. temperat. /K	120(1)	120(1)
q range /°	2.5 to 71.2	2.2 to 28.3
index ranges *h*,*k*,*l*	-21 ... 21, -27 ... 27, -21 ... 21	-13 ... 13, -24 ... 24, -29 ... 29
reflections measured	189925	69147
unique [R_{int}]	13371 [0.0716]	9957 [0.0675]
observed [*I*≥2s(*I*)]	10854	6775
data / restraints /parameters	13371 / 45 / 1079	9957 / 0 / 638
GooF on F^2	1.022	1.012
R indices [*F*>4s(*F*)] *R*(*F*), *wR*(F^2)	0.0734, 0.1981	0.0405, 0.0844
R indices (all data) *R*(*F*), *wR*(F^2)	0.0871, 0.2112	0.0786, 0.0981
largest residual peaks /e⋅Å^{-3}	0.916, -1.150	0.399, -0.430
instrument	Supernova	Kappa CCD
structure solution	SIR2014 (VLD)	SHELXT
deposition number CCDC	1915081	1915082

[a] numerical absorption correction. [b] semi-empirical absorption correction.

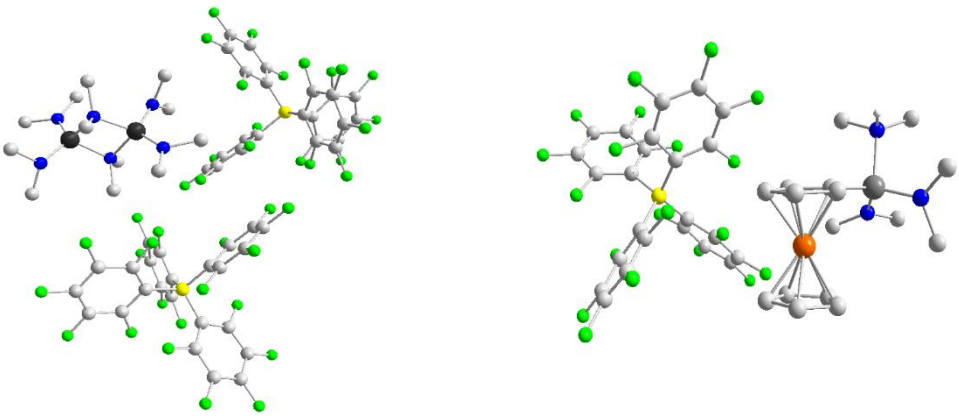

Figure SI 2: Solid state structures of [**1**][B(C_6F_5)$_4$]$_2$·2CH_2Cl_2 (left, solvent omitted for clarity) and [2a][B(C_6F_5)$_4$)] (right).

6. Spectra

6.1. [(NMe$_2$)$_3$Si]$_2$[B(C_6F_5)$_4$]$_2$ [1]

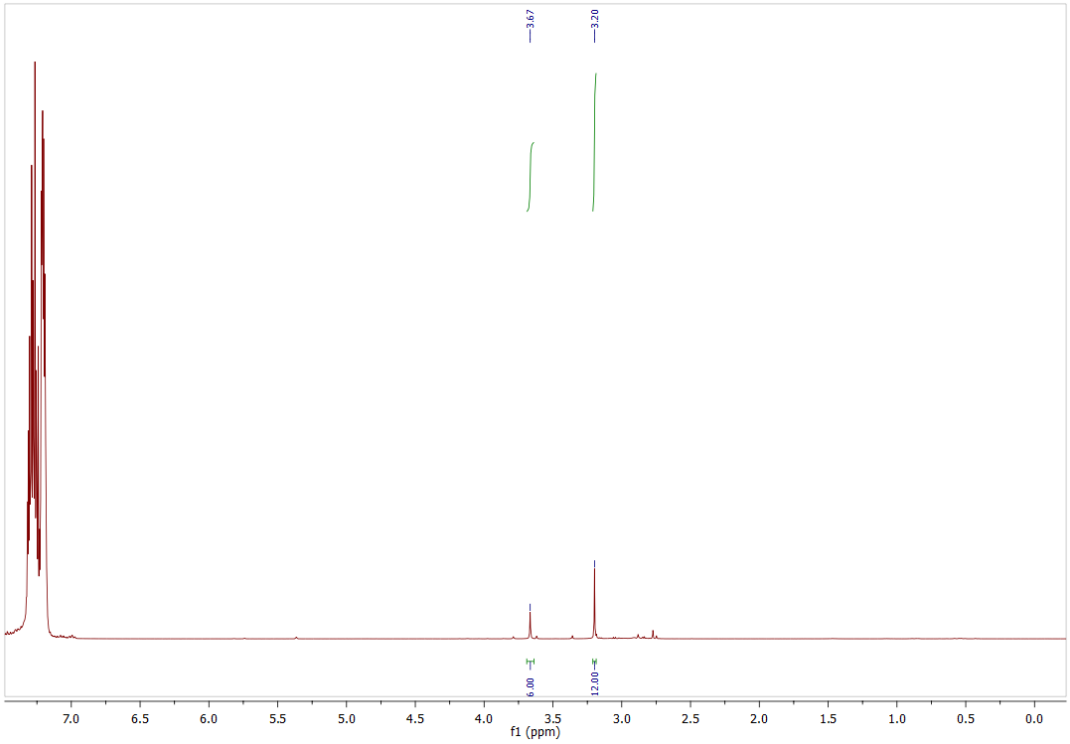

Figure SI 3: ^{1}H-NMR spectrum of **[1]**[B(C_6F_5)$_4$]$_2$ in *o*-difluorobenzene.

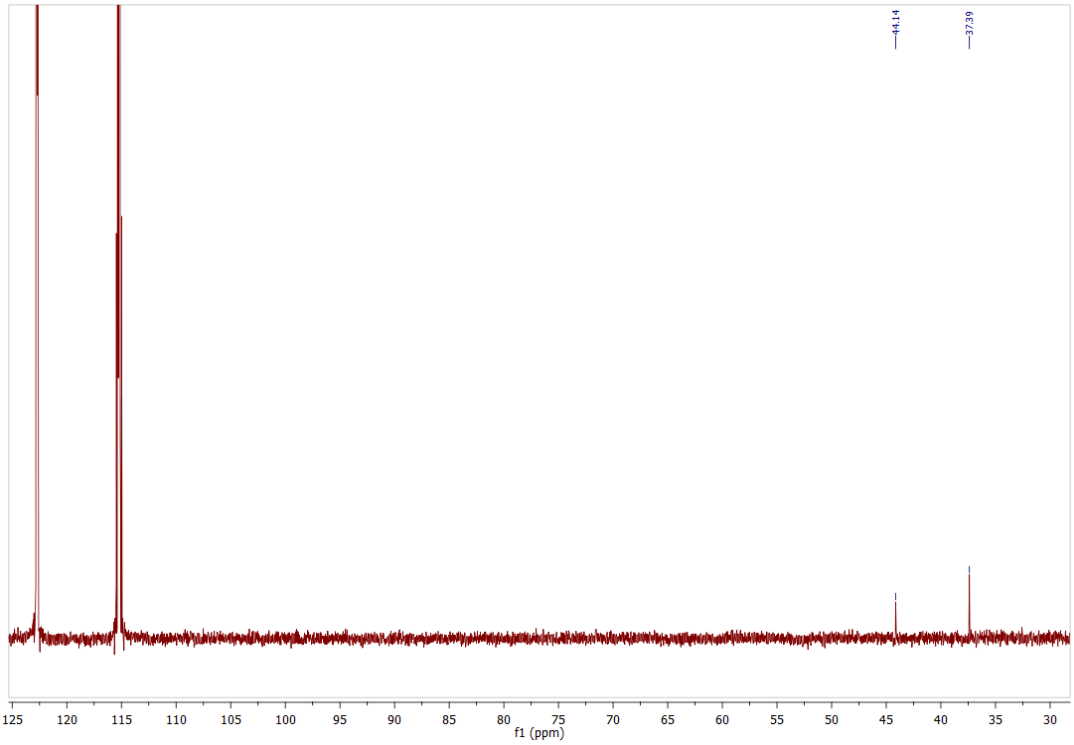

Figure SI 4: $^{13}C\{^{1}H\}$-NMR spectrum of **[1]**$[B(C_6F_5)_4]_2$ in *o*-difluorobenzene.

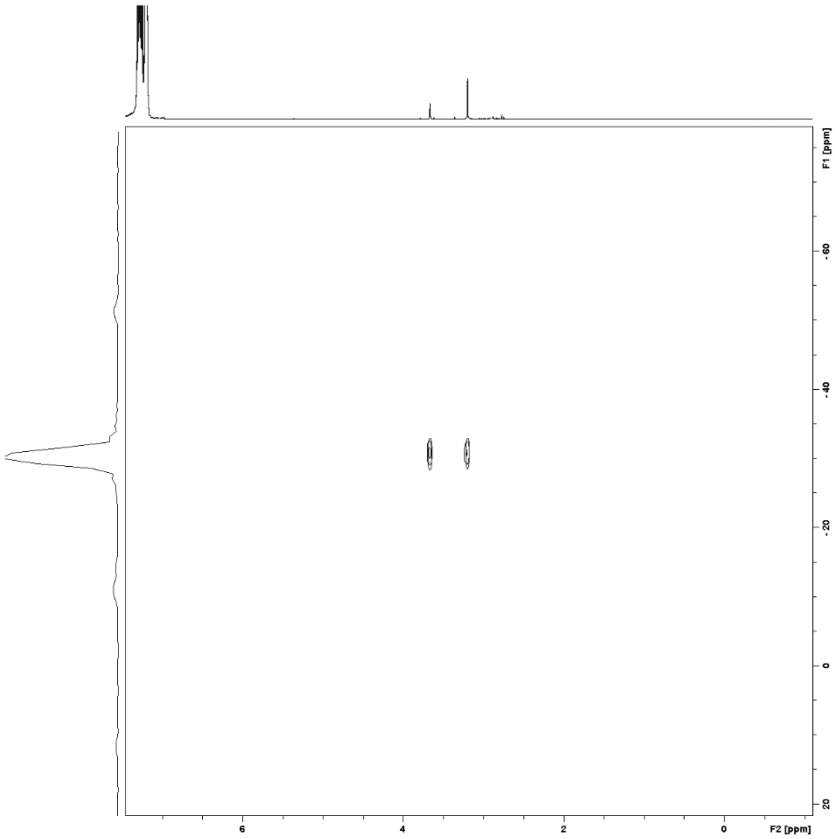

Figure SI 5: $^{1}H/^{29}Si$-HMBC-NMR spectrum of **[1]**$[B(C_6F_5)_4]_2$ in *o*-difluorobenzene.

6.2. $[(NMe_2)_3Si(OPEt_3)]\ [B(C_6F_5)_4]$

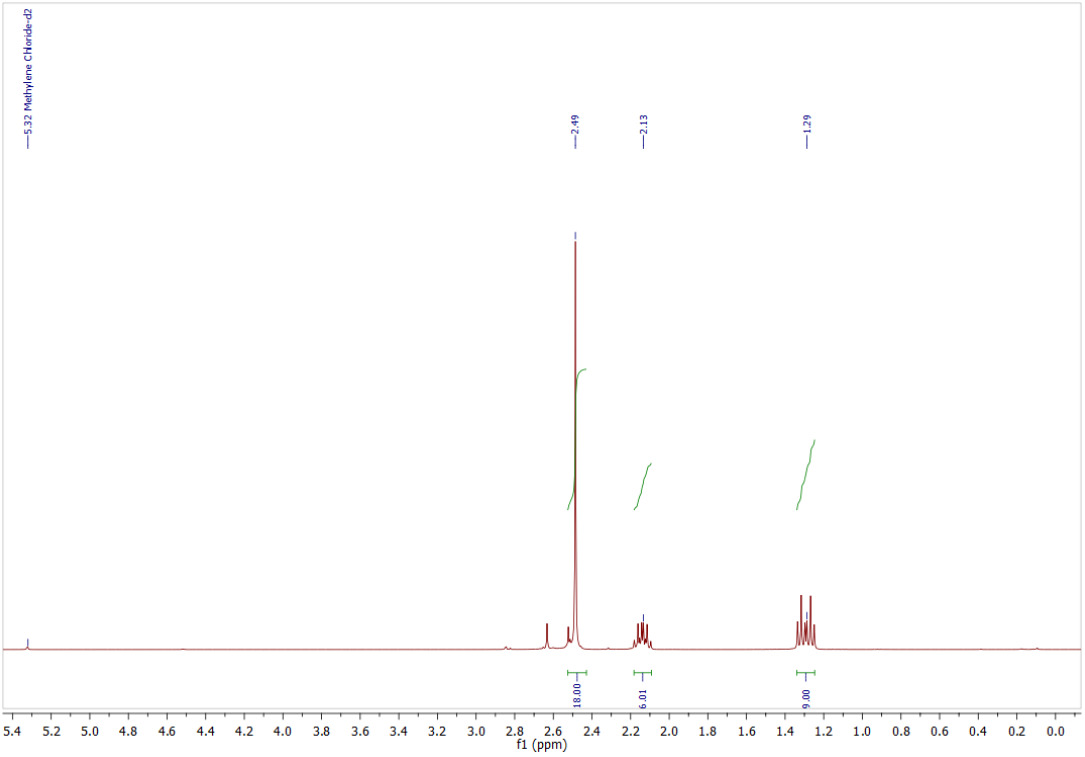

Figure SI 6: ^{1}H-NMR spectrum of $[(NMe_2)_3Si(OPEt_3)][B(C_6F_5)_4]$ in dichloromethane-d_2.

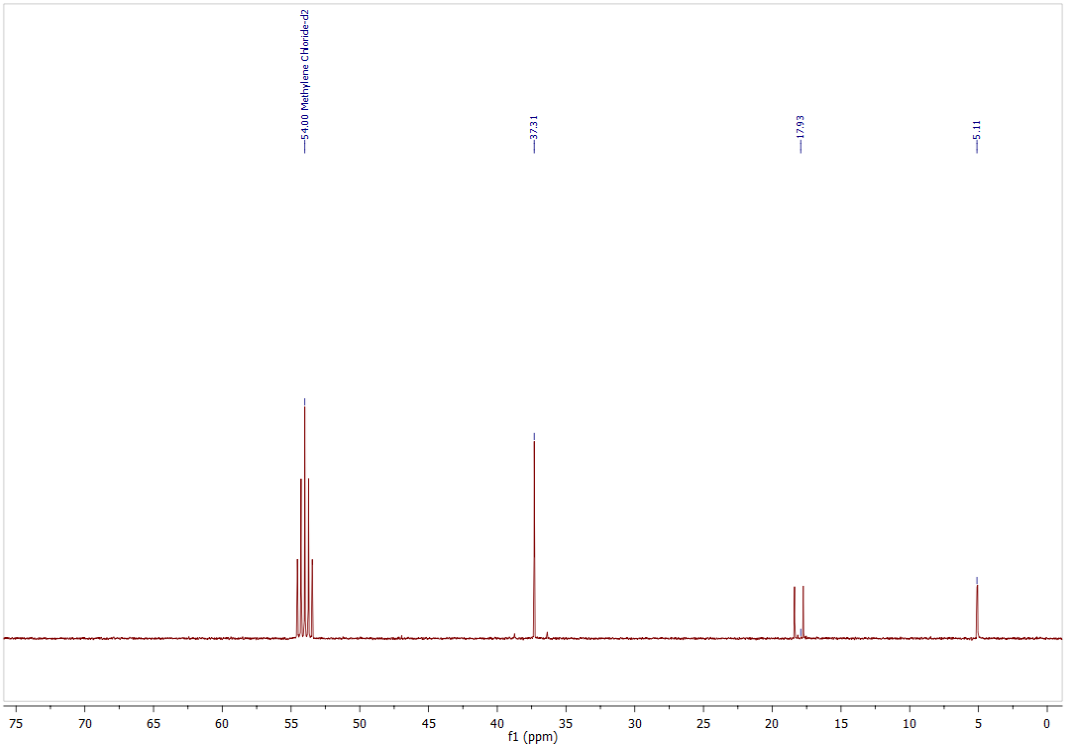

Figure SI 7: $^{13}C\{^{1}H\}$-NMR spectrum of $[(NMe_2)_3Si(OPEt_3)][B(C_6F_5)_4]$ in dichloromethane-d_2.

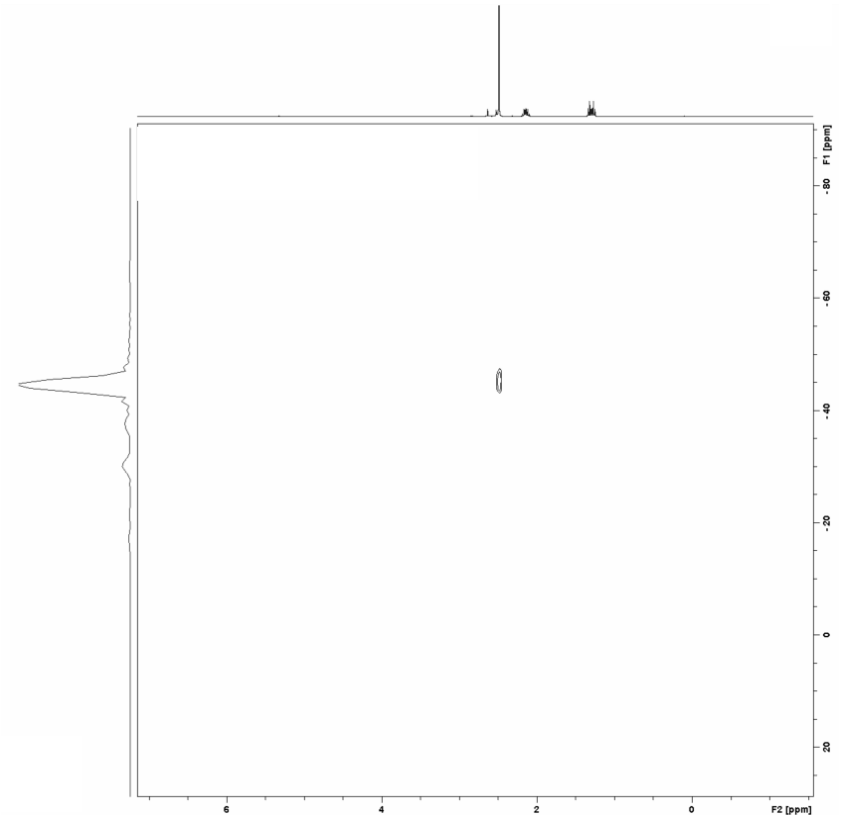

Figure SI 8: $^{1}H/^{29}Si$-HMBC-NMR spectrum of $[(NMe_2)_3Si(OPEt_3)][B(C_6F_5)_4]$ in dichloromethane-d_2.

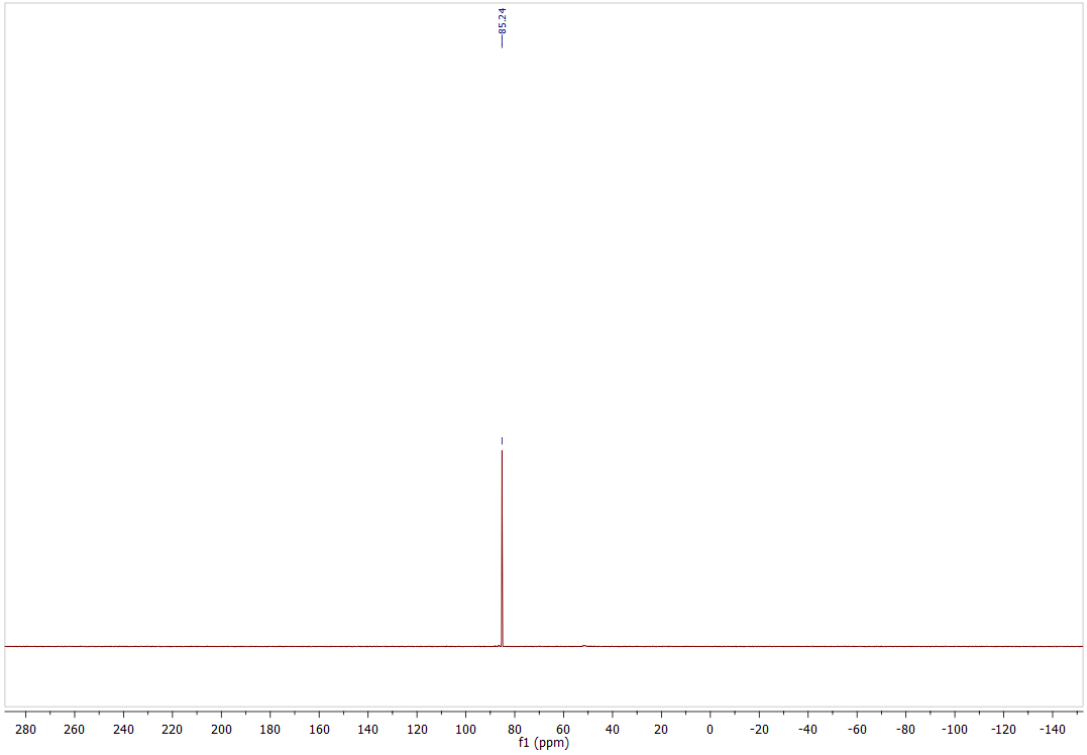

Figure SI 9: $^{31}P\{^{1}H\}$-NMR spectrum of $[(NMe_2)_3Si(OPEt_3)][B(C_6F_5)_4]$ in dichloromethane-d_2.

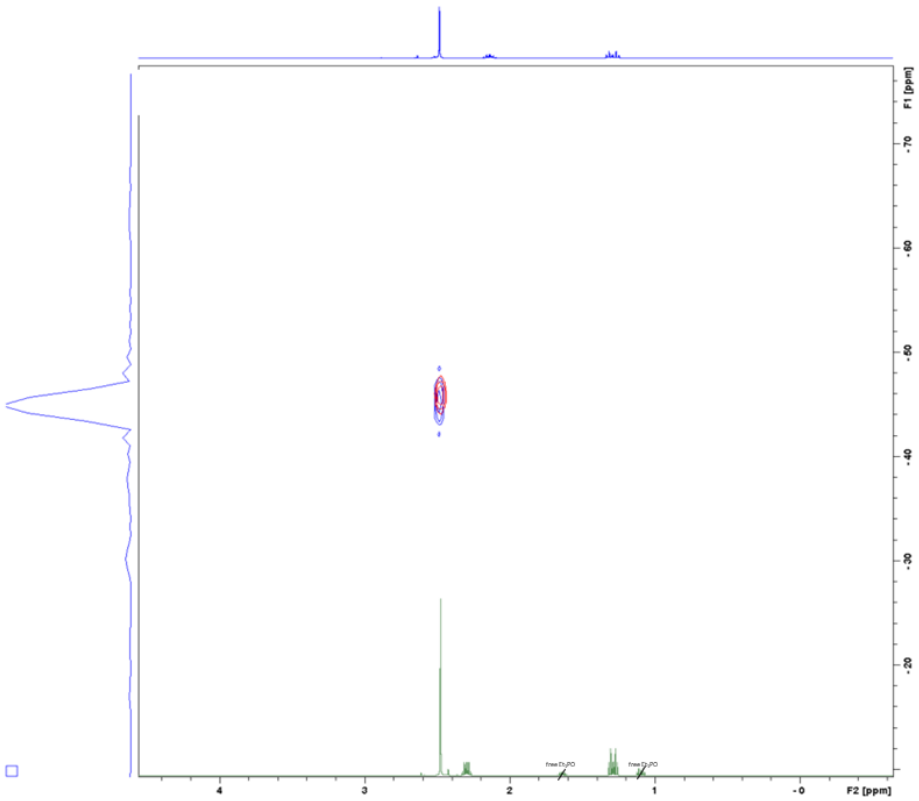

Figure SI 10: $^{1}H/^{29}Si$-HMBC-NMR spectrum of $[(NMe_2)_3Si(OPEt_3)][B(C_6F_5)_4]$ (blue) compared to $[(NMe_2)_3Si(OPEt_3)][OTf]$ (green, red) in dichloromethane-d_2.

6.3. Ferrocenyl-bis-dimethylamino(dimethylammonium)silyl $[(B(C_6F_5)_4]$ / [2a]$[(B(C_6F_5)_4]$

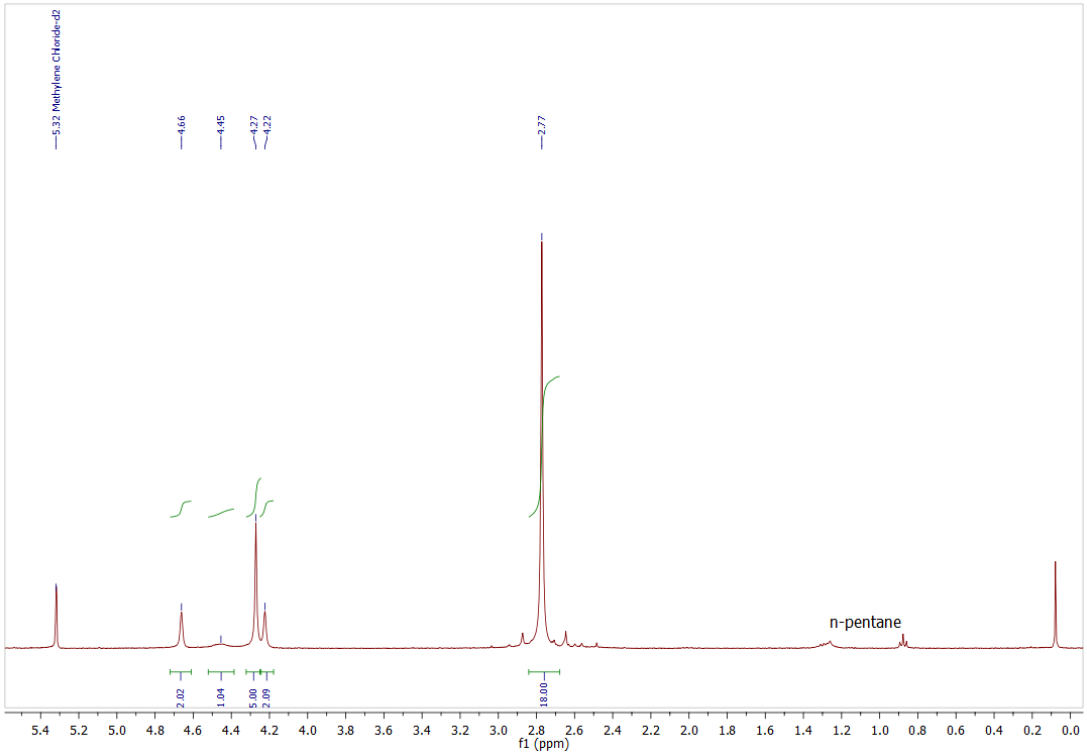

Figure SI 11: ^{1}H-NMR spectrum of **[2a]**$[B(C_6F_5)_4]$ in dichloromethane-d_2.

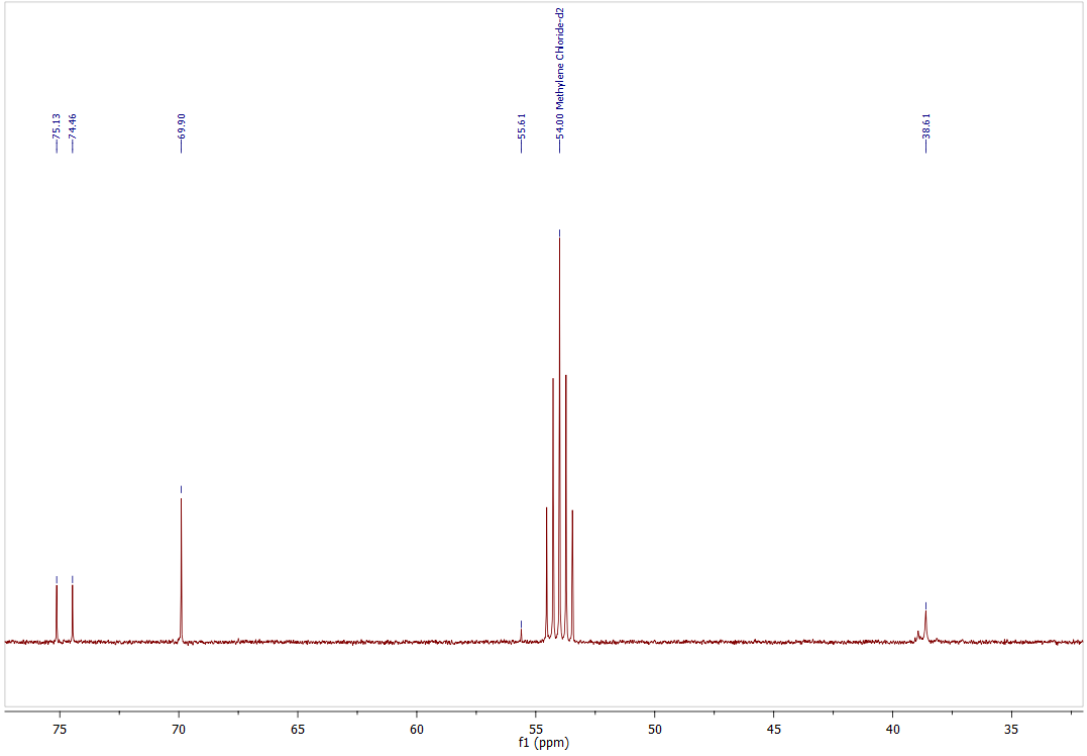

Figure SI 12: $^{13}C\{^{1}H\}$-NMR spectrum of **[2a]**[$B(C_6F_5)_4$] in dichloromethane-d_2.

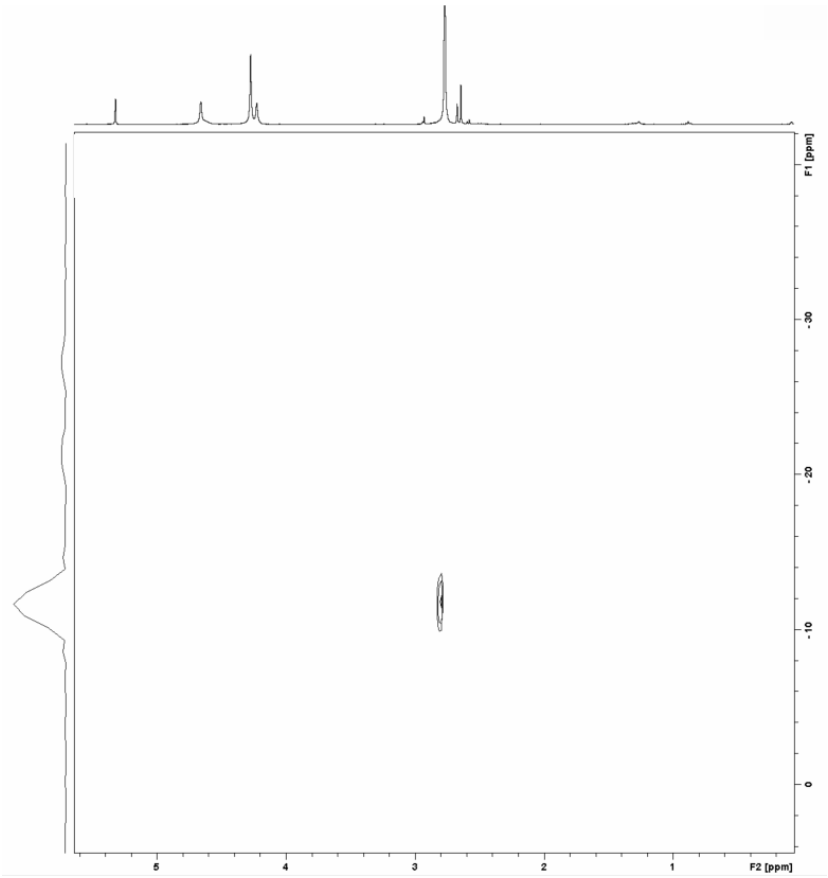

Figure SI 13: $^{1}H/^{29}Si$-HMBC-NMR spectrum of **[2a]**[$B(C_6F_5)_4$] in dichloromethane-d_2.

6.4. 1-Methyl-3-tris-dimethylaminosilylindole [(B(C_6F_5)$_4$] / [2b][(B(C_6F_5)$_4$]

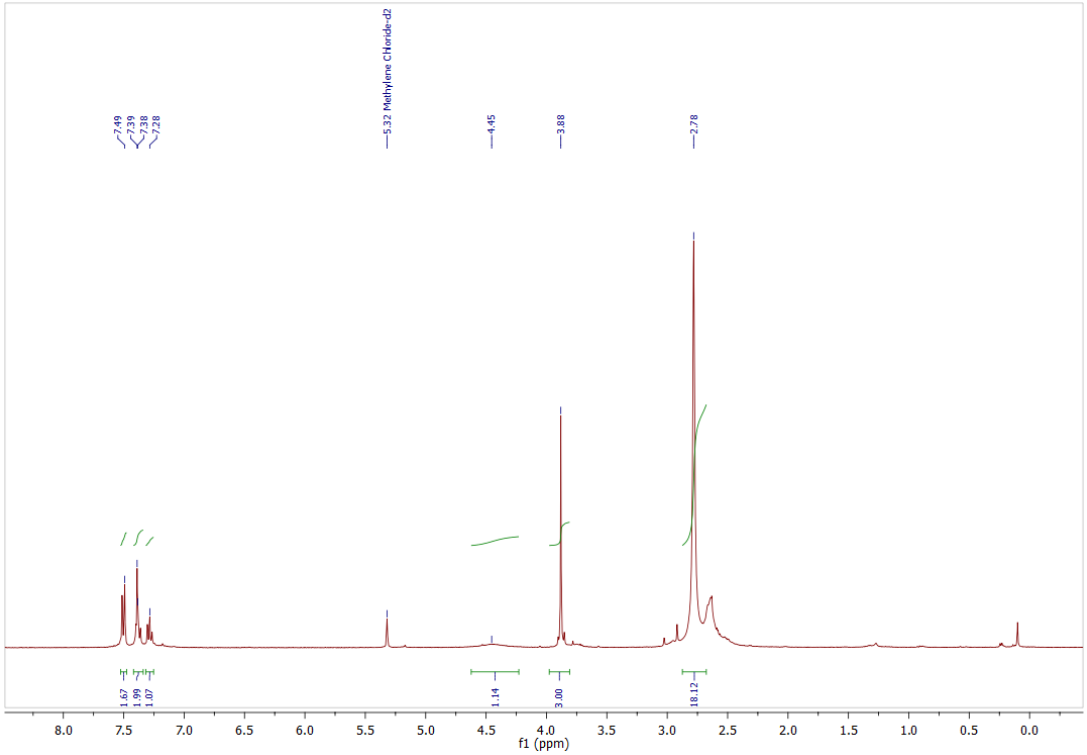

Figure SI 14: ^{1}H-NMR spectrum of **[2b]**[B(C_6F_5)$_4$] in dichloromethane-d_2.

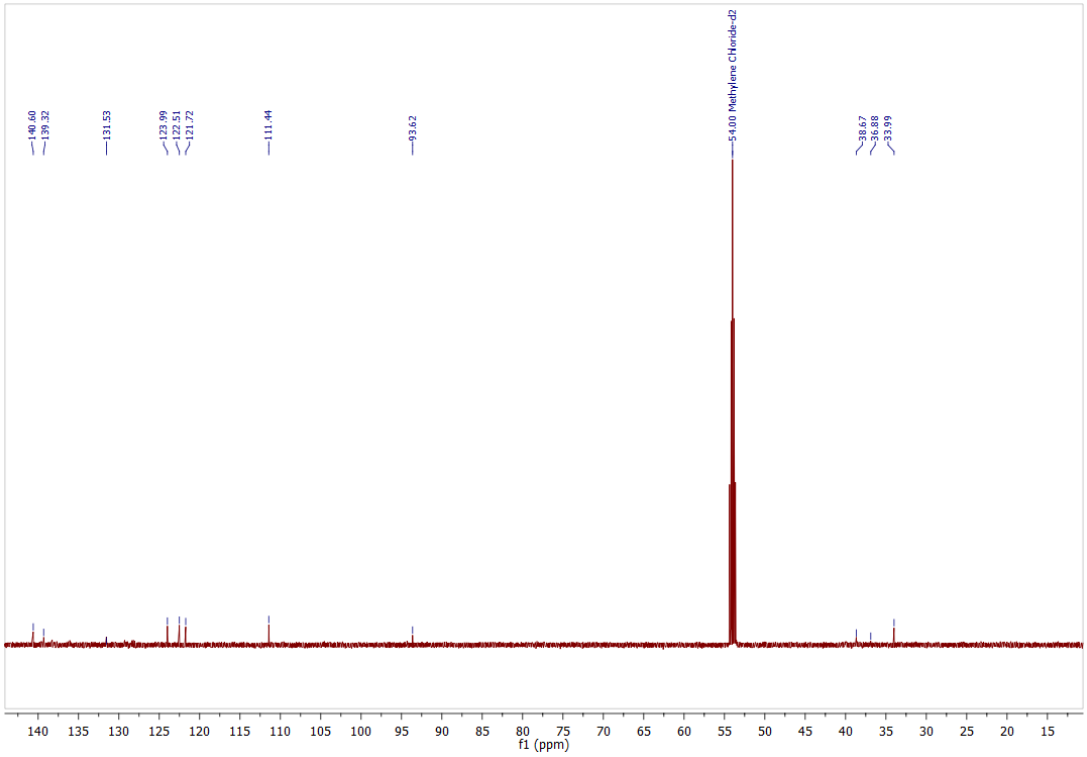

Figure SI 15: ^{13}C{^{1}H}-NMR spectrum of **[2b]**[B(C_6F_5)$_4$] in dichloromethane-d_2.

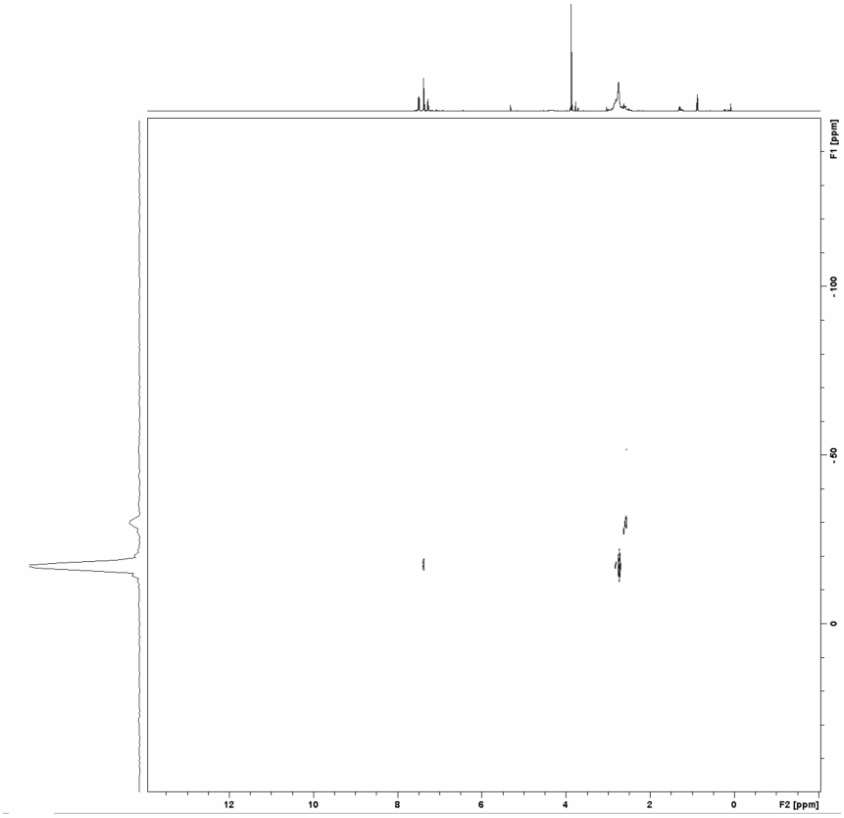

Figure SI 16: $^{1}H/^{29}Si$-HMBC-NMR spectrum of **[2b]**[$B(C_6F_5)_4$] in dichloromethane-d_2.

6.5. *N,N*-Dimethyl-4-bis(dimethylamino)(dimethylammonium)silylbenzamine [($B(C_6F_5)_4$] / [2c] [($B(C_6F_5)_4$]

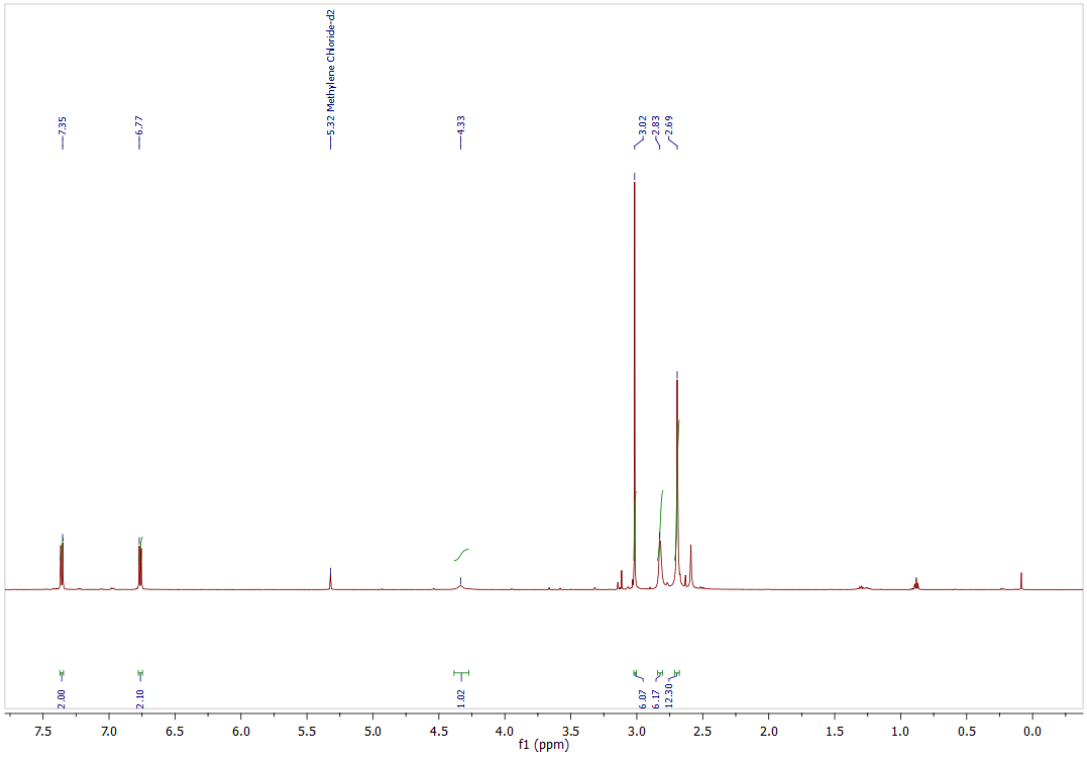

Figure SI 17: ^{1}H-NMR spectrum of **[2c]**[$B(C_6F_5)_4$] in dichloromethane-d_2.

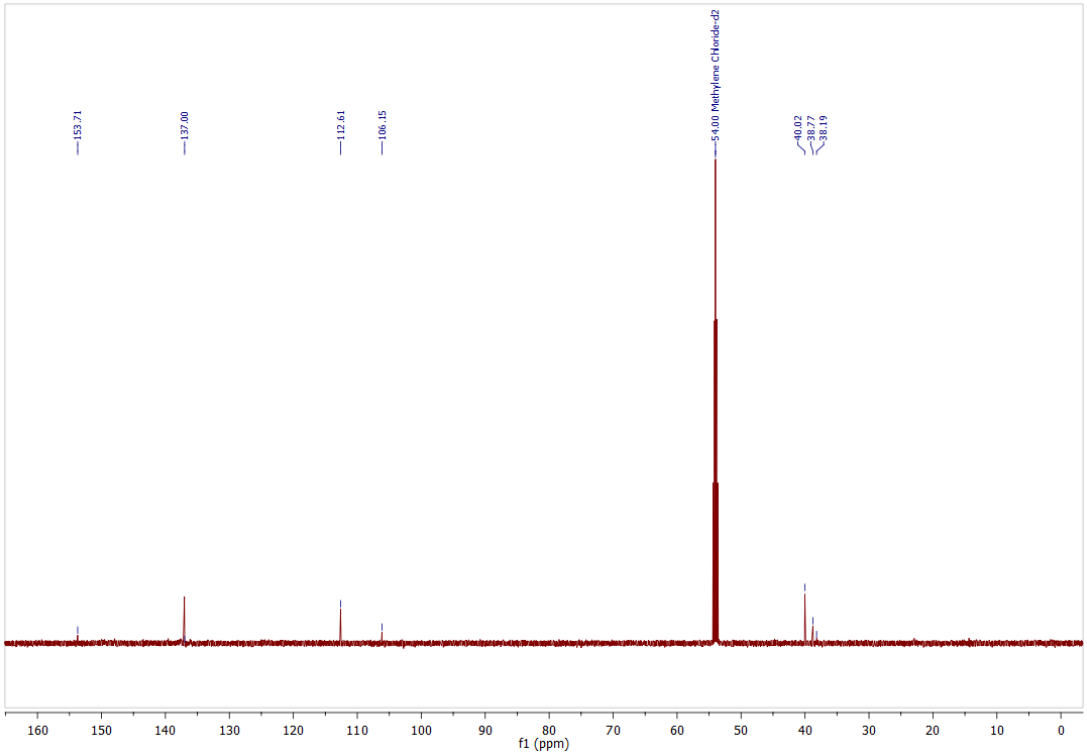

Figure SI 18: $^{13}C\{^{1}H\}$-NMR spectrum of **[2c]**[$B(C_6F_5)_4$] in dichloromethane-d_2.

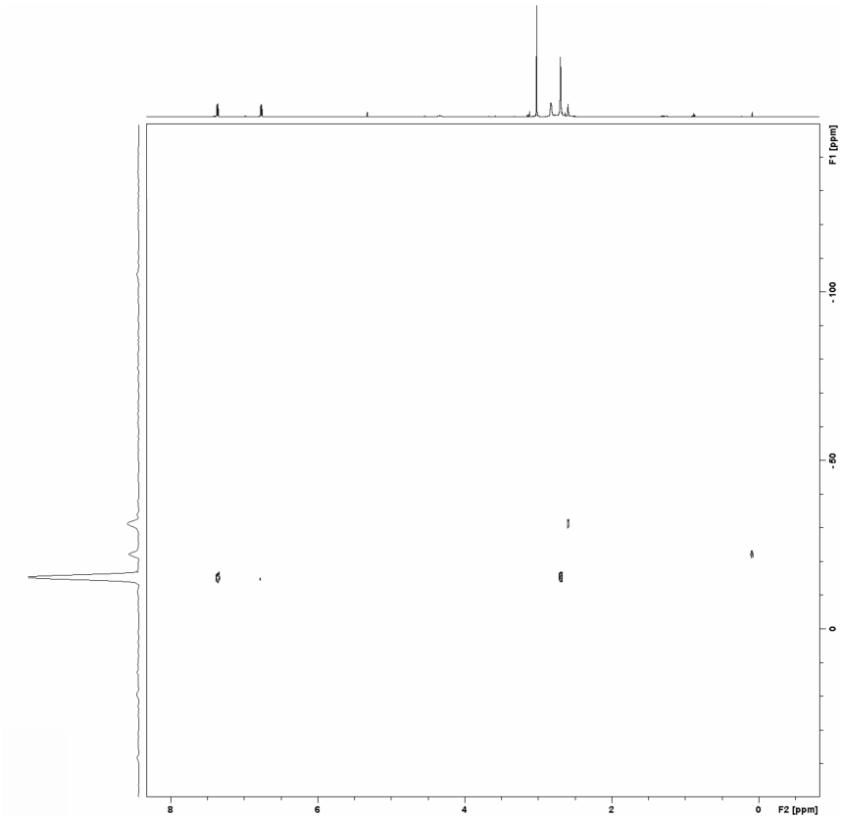

Figure SI 19: $^{1}H/^{29}Si$-HMBC-NMR spectrum of **[2c]**[$B(C_6F_5)_4$] in dichloromethane-d_2.

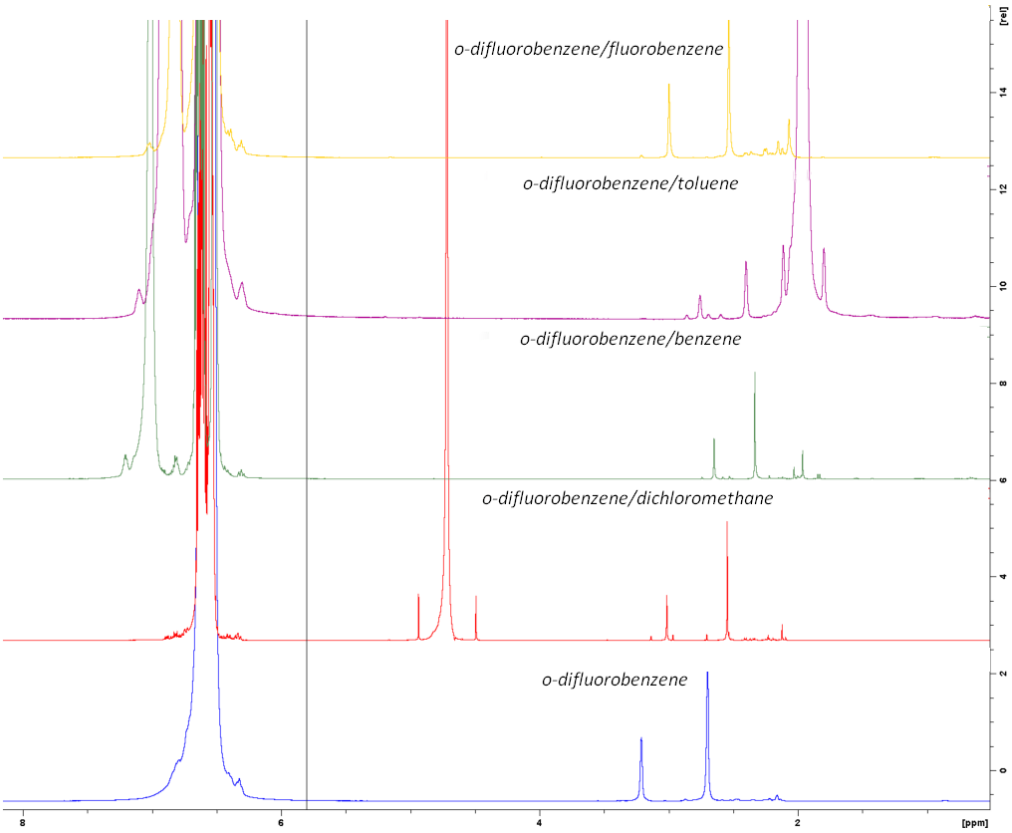

Figure SI 20: ^{1}H-NMR spectra of **[1]**[(B(C_6F_5)$_4$]$_2$ in *o*-difluorobenzene/solvent mixtures and the change in the chemical shift referenced on the shift in *o*-difluorobenzene as standard.

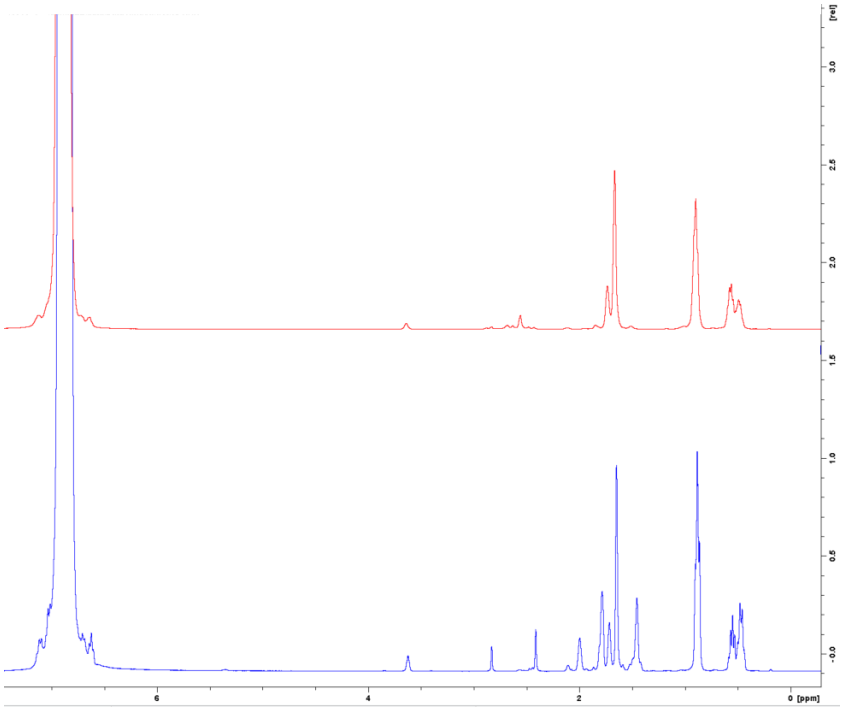

Figure SI 21: ^{1}H-NMR spectra of the conversion from 1-fluoroadamantane to adamantane in o-difluorobenzene, initiated by **[1]**[(B(C_6F_5)$_4$]$_2$, after 30 min (blue) and <12 h (red).

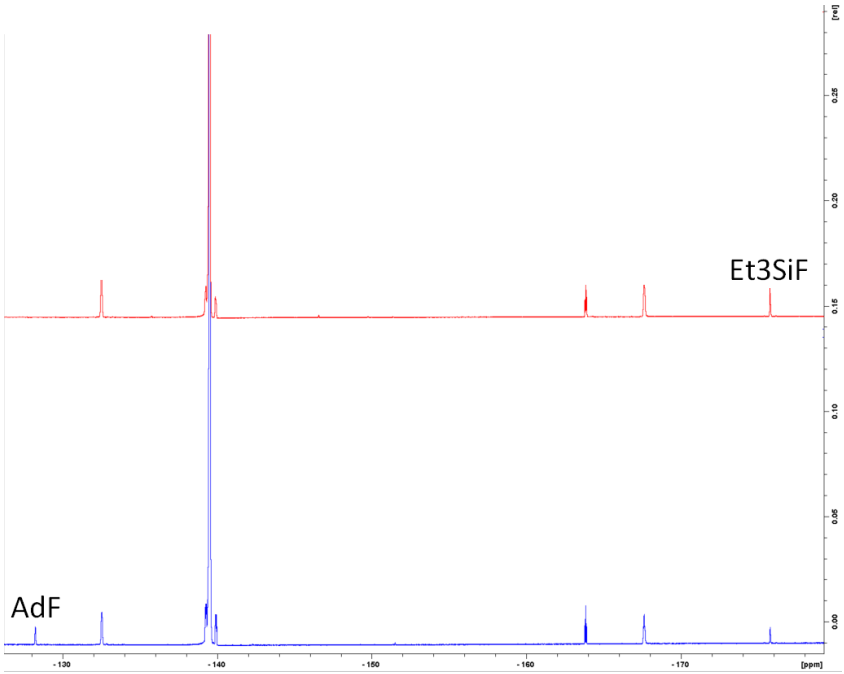

Figure SI 22: ^{19}F-NMR spectra of the conversion from 1-fluoroadamantane to adamantane *o*-difluorobenzene, initiated by **[1]**[(B(C_6F_5)$_4$]$_2$, after 30 min (blue) and <12 h (red).

References

[1] a) F. Neese, *Wiley Interdisc. Rev: Comp. Mol. Sci.* **2012**, *2*, 73-78; b) F. Neese, *Wiley Interdisciplinary Reviews: Computational Molecular Science* **2017**, e1327-n/a.

[2] K. Eichkorn, O. Treutler, H. Öhm, M. Häser, R. Ahlrichs, *Chem. Phys. Lett.* **1995**, *240*, 283-290.

[3] K. Eichkorn, F. Weigend, O. Treutler, R. Ahlrichs, *Theor. Chem. Acc.* **1997**, *97*, 119-124.

[4] Y. Zhao, D. G. Truhlar, *J. Phys. Chem. A* **2005**, *109*, 5656-5667.

[5] S. Grimme, J. Antony, S. Ehrlich, H. Krieg, *J. Chem. Phys.* **2010**, *132*, 154104.

[6] a) S. Grimme, S. Ehrlich, L. Goerigk, *J. Comput. Chem.* **2011**, *32*, 1456-1465; b) A. D. Becke, E. R. Johnson, *J. Chem. Phys.* **2005**, *122*, 154104; c) E. R. Johnson, A. D. Becke, *J. Chem. Phys.* **2005**, *123*, 024101.

[7] a) A. Schäfer, C. Huber, R. Ahlrichs, *J. Chem. Phys.* **1994**, *100*, 5829-5835; b) F. Weigend, R. Ahlrichs, *Phys. Chem. Chem. Phys.* **2005**, *7*, 3297-3305.

[8] S. Grimme, *Chem. Eur. J.* **2012**, *18*, 9955-9964.

[9] a) F. Neese, A. Hansen, D. G. Liakos, *J. Chem. Phys.* **2009**, *131*, 064103; b) C. Riplinger, F. Neese, *J. Chem. Phys.* **2013**, *138*, 034106; c) C. Riplinger, B. Sandhoefer, A. Hansen, F. Neese, *J. Chem. Phys.* **2013**, *139*, 134101.

[10] E. Paulechka, A. Kazakov, *J. Phys. Chem. A* **2017**, *121*, 4379-4387.

[11] a) R. A. Kendall, T. H. Dunning, R. J. Harrison, *J. Chem. Phys.* **1992**, *96*, 6796-6806; b) B. P. Prascher, D. E. Woon, K. A. Peterson, T. H. Dunning, A. K. Wilson, *Theor. Chem. Acc.* **2011**, *128*, 69-82; c) D. E. Woon, T. H. Dunning, *J. Chem. Phys.* **1993**, *98*, 1358-1371; d) F. Weigend, A. Köhn, C. Hättig, *J. Chem. Phys.* **2002**, *116*, 3175-3183; e) K. A. Peterson, C. Puzzarini, *Theor. Chem. Acc.* **2005**, *114*, 283-296.

[12] G. Bistoni, A. A. Auer, F. Neese, *Chem. Eur. J.* **2017**, *23*, 865-873.

[13] a) A. Klamt, *J. Phys. Chem.* **1995**, *99*, 2224-2235; b) F. Eckert, A. Klamt, *AlChE J.* **2002**, *48*, 369-385; c) A. Klamt, B. Mennucci, J. Tomasi, V. Barone, C. Curutchet, M. Orozco, F. J. Luque, *Acc. Chem. Res.* **2009**, *42*, 489-492.

[14] E. J. Baerends, T. Ziegler, A. J. Atkins, J. Autschbach, D. Bashford, O. Baseggio, A. Brces, F. M. Bickelhaupt, C. Bo, P. M. Boerritger, L. Cavallo, C. Daul, D. P. Chong, D. V. Chulhai, L. Deng, R. M. Dickson, J. M. Dieterich, D. E. Ellis, M. van Faassen, A. Ghysels, A. Giammona, S. J. A. van Gisbergen, A. Goez, A. W. Gtz, S. Gusarov, F. E. Harris, P. van den Hoek, Z. Hu, C. R. Jacob, H. Jacobsen, L. Jensen, L. Joubert, J. W. Kaminski, G. van Kessel, C. Knig, F. Kootstra, A. Kovalenko, M. Krykunov, E. van Lenthe, D. A. McCormack, A. Michalak, M. Mitoraj, S. M. Morton, J. Neugebauer, V. P. Nicu, L. Noodleman, V. P. Osinga, S. Patchkovskii, M. Pavanello, C. A. Peeples, P. H. T. Philipsen, D. Post, C. C. Pye, H. Ramanantoanina, P. Ramos, W. Ravenek, J. I. Rodrguez, P. Ros, R. Rger, P. R. T. Schipper, D. Schlns, H. van Schoot, G. Schreckenbach, J. S. Seldenthuis, M. Seth, J. G. Snijders, Sol.

[15] E. Van Lenthe, E. J. Baerends, *J. Comput. Chem.* **2003**, *24*, 1142-1156.

[16] J. Tomasi, B. Mennucci, R. Cammi, *Chem. Rev.* **2005**, *105*, 2999-3094.

[17] R. Franke, B. Hannebauer, *Phys. Chem. Chem. Phys.* **2011**, *13*, 21344-21350.

[18] N. W. Mitzel, K. Vojinović, R. Fröhlich, T. Foerster, H. E. Robertson, K. B. Borisenko, D. W. H. Rankin, *J. Am. Chem. Soc.* **2005**, *127*, 13705-13713.

[19] M. Mitoraj, A. Michalak, *J. Mol. Model.* **2008**, *14*, 681-687.

[20] T. Ziegler, A. Rauk, *Theo. chim. act.* **1977**, *46*, 1-10.

[21] M. P. Mitoraj, A. Michalak, T. Ziegler, *J. Chem. Theo. Comp.* **2009**, *5*, 962-975.

[22] J. Molina Molina, J. A. Dobado, *Theor. Chem. Acc.* **2001**, *105*, 328-337.

[23] O. V. Dolomanov, L. J. Bourhis, R. J. Gildea, J. A. K. Howard, H. Puschmann, *J. Appl. Crystallogr.* **2009**, *42*, 339-341.

[24] G. M. S. U. o. G. G. Sheldrick, Germany.

[25] Kabsch, K. in: Rossmann, M. G., Arnold, E. (eds.) *"International Tables for Crystallography" Vol. F*, Ch. 11.3, Kluwer Academic Publishers, Dordrecht, The Netherlands **2001**.

[26] Otwinowski, Z. *denzo*, **1985-94**.

[27] *CrysAlisPro*, Agilent Technologies UK Ltd., Oxford, UK **2011-2014** and Rigaku Oxford Diffraction, Rigaku Polska Sp.z o.o., Wrocław, Poland **2015-2018**.

[28] Blessing, R. H. *Acta Cryst.* **1995**, *A51*, 33.

[29] Otwinowski, Z. *scalepack*, **1985-94**.

[30] *SCALE3 ABSPACK, CrysAlisPro*, Agilent Technologies UK Ltd., Oxford, UK **2011-2014** and Rigaku Oxford Diffraction, Rigaku Polska Sp.z o.o., Wrocław, Poland **2015-2018**.

[31] a) Sheldrick, G. M. *SADABS*, Bruker AXS GmbH, Karlsruhe, Germany **2004-2014**; (b) Krause, L; Herbst-Irmer, R.; Sheldrick, G. M.; Stalke, D. *J. Appl. Cryst.* **2015**, *48*, 3.

[32] W. R. Busing, H. A. Levy, *Acta Cryst.* **1957**, *10*, 180.

[33] (a) G. M. Sheldrick, *SHELXT*, University of Göttingen and Bruker AXS GmbH, Karlsruhe, Germany, **2012-2018**; (b) M. Ruf, B. C. Noll, *Application Note SC-XRD 503*, Bruker AXS GmbH, Karlsruhe, Germany, **2014**; (c) G. M. Sheldrick, *Acta Cryst.* **2015**, *A71*, 3.

[34] (a) M. C. Burla, R. Caliandro, B. Carrozzini, G. L. Cascarano, C. Cuocci, C. Giacovazzo, M. Mallamo, A. Mazzone, G. Polidori, *SIR2014*, CNR IC, Bari, Italy, **2014**; (b) M. C. Burla, R. Caliandro, B. Carrozzini, G. L. Cascarano, C. Cuocci, C. Giacovazzo, M. Mallamo, A. Mazzone, G. Polidori, *J. Appl. Cryst.* **2015**, *48*, 306.

[35] (a) Sheldrick, G. M. *SHELXL-20xx*, University of Göttingen and Bruker AXS GmbH, Karlsruhe, Germany **2012-2018**; (b) Sheldrick, G. M. *Acta Cryst.* **2008**, *A64*, 112; (c) Sheldrick, G. M. *Acta Cryst.* **2015**, *C71*, 3.

[36] (a) J. S. Rollett in: F. R. Ahmed, S. R. Hall, C. P. Huber (eds.) *„Crystallographic Computing"* p. 167, Munksgaard, Copenhagen, Denmark, **1970**; (b) D. Watkin in: N. W. Isaaks, M. R. Taylor (eds.) *„Crystallographic Computing 4"*, Ch. 8, IUCr and Oxford University Press, Oxford, UK, **1988**; (c) P. Müller, R. Herbst-Irmer, A. L. Spek, T. R. Schneider, M. R. Sawaya in: P. Müller (ed.) *"Crystal Structure Refinement"*, Ch. 5, Oxford University Press, Oxford, UK, **2006**; (d) D. Watkin, *J. Appl. Cryst.* **2008**, *41*, 491.